Estimating Water Transparency in a Shallow Hypertrophic Lagoon (Albufera of Valencia, Spain) Using Sentinel-2 Images

Juan V. Molner , Juan M. Soria * , Rebeca Pérez-González , Xavier Sòria-Perpinyà

Posted Date: 6 September 2023

doi: 10.20944/preprints202309.0311.v1

Keywords: Secchi disk depth; water quality; remote sensing; eutrophication; optical modeling; water management

Article

Estimating Water Transparency in a Shallow Hypertrophic Lagoon (Albufera of Valencia, Spain) Using Sentinel-2 Images

Juan V. Molner [1], Juan M. Soria [1,*], Rebeca Pérez-González [1] and Xavier Sòria-Perpinyà [2]

[1] Cavanilles Institute of Biodiversity and Evolutionary Biology (ICBiBE), Universitat de València, 46980 Valencia, Spain; molpo@alumni.uv.es (J.V.M.); repegon@alumni.uv.es (R.P.-G.)
[2] Image Processing Laboratory (IPL), Universitat de València, 46980 València, Spain; javier.soria-perpina@uv.es (X.S.-P.)
* Correspondence: juan.soria@uv.es

Abstract: In this study, we investigated water transparency estimation models in the hypertrophic lagoon of the Albufera of Valencia using Sentinel-2 images. Water transparency, a crucial environmental indicator, was assessed via Secchi disk depth (Z_{SD}) measurements. Three optical models (R490/R560, R490/R705, R560/R705) were explored to establish a robust algorithm for Z_{SD} estimation. Through extensive field sampling and laboratory analyses, weekly data spanning 2018 to 2023 were collected, including water transparency, temperature, conductivity, and chlorophyll-a concentration. Remote sensing imagery from the Sentinel-2 mission was employed, and images were processed using SNAP software. The R560/R705 model, calibrated for turbid lakes, emerged as the most suitable. The algorithm's calibration was validated with high correlation coefficients (R^2) in both calibration (0.6149) and validation (0.916) phases, demonstrating the model's accuracy in estimating Z_{SD}. This new algorithm significantly outperformed a previous approach, highlighting the importance of tailoring algorithms to specific water body characteristics. The study contributes to improved water quality assessment and resource management, underscoring the value of remote sensing in environmental research.

Keywords: Secchi disk depth; water quality; remote sensing; eutrophication; optical modeling; water management

1. Introduction

Water clarity is the first characteristic of water that humans perceive, related to water transparency and turbidity [1]. Water transparency could be defined as the extinction of light along the water column, conventionally estimated by Secchi disk depth (Z_{SD}) [2]. Using this instrument, what is measured is the distance it travels vertically until it is no longer visible to the human eye [3,4], this measurement being a good indicator of the depth at which sunlight penetrates the water [5].

An important symptom of eutrophication is the reduction of light penetration through the water column via elevated phytoplankton and sediment biomass [6] and can profoundly affect photosynthesis and photorespiration [7]. Thus, Z_{SD} is inversely related to the average amount of inorganic and organic material in the water [4].

One of the tools that has proven to be very useful in monitoring these variables is remote sensing [8], with water transparency or Z_{SD} being one of the variables that are usually estimated using remote sensing data for monitoring water bodies [9]. In addition, Z_{SD} is one of the variables that allow the establishment of the trophic status of water bodies [10] and the ecological status according to the criteria of the Water Framework Directive [11].

Through remote sensing studies, it has been shown that water transparency decreases with increasing reflectivity in the red region of the spectrum due to light scattering by coarse suspended particles [1]. Furthermore, as mentioned in Caballero et al. [12], the near-infrared region is also sensitive to high concentrations of suspended solids.

 doi:10.20944/preprints202309.0311.v1

In this sense, remote sensing data, with its ability to obtain a synoptic view, repetitive coverage with sensors calibrated to detect changes and observations at different resolutions, offer a better alternative for natural resource management compared to traditional methods [13]. However, work on water transparency by remote sensing has been scarce. Subsequently, Sentinel-2 arrived, an ESA mission consisting of the S2A and S2B satellites, which generate images with better spectral resolution (up to 10 m) and shorter revisit time (5 days) than previous satellites [14].

In this context, the Ecological Status of AQuatic Systems with Sentinel Satellites (ESAQS) project was approved in 2016, with the main objective of developing and validating algorithms for the estimation of ecological indicators of quality in inland waters, including chlorophyll-a [Chl-a] concentration, transparency, dissolved organic matter and suspended solids, from S2 images in different lakes and reservoirs of the Jucar basin [15].

In the framework of this project, Pereira-Sandoval et al. [15] developed an algorithm, based on the ratio between the reflectances at 490 nm and 705 nm, to estimate the Z_{SD} in turbid waters with Sentinel-2 images, calibrated from data from the Albufera and different reservoirs in the Valencian Community. Delegido et al. [16] obtained a new algorithm for obtaining the Z_{SD} but based on the ratio between the reflectances at 490 nm and 560 nm. Subsequently, Sòria-Perpinyà et al. [17] validated a different algorithm to estimate the Z_{SD}, based on the ratio between the reflectances at 560 and 705 nm, calibrated for the Albufera of Valencia from S2 images. However, with the progressive decrease of water clarity in the Albufera of Valencia due to the advance of eutrophication, the estimates of this algorithm are deviating by 20% from the real values measured in situ.

Accordingly with this line of research, the main objective of this study has been to develop a new algorithm to estimate the Secchi Disk Depth (Z_{SD}) in the Albufera lagoon, evaluating previous optical models. This initiative is directly aligned with Sustainable Development Goal number 6 (SDG 6), which promotes the availability and sustainable management of water and sanitation for all. The search for efficient and accurate methods to assess water quality in an ecosystem as significant as the Albufera lagoon contributes to the achievement of broader goals related to sustainable management of water resources and conservation of aquatic ecosystems.

2. Materials and Methods

2.1. Study area

The Albufera of Valencia is a Mediterranean coastal lagoon located at 39.335° N, -0.335° W, known for its oligohaline nature with a salinity of 1-2 ‰ and shallow depth of 1.2 m [18,19]. This unique environment boasts significant biodiversity and holds immense historical, cultural, and scenic value warranting conservation efforts. Recognized as the first Natural Park designated in the Valencian Community in 1986, it also forms an integral part of the Natura 2000 Network, designated as a "Site of Community Importance" (SCI) since 2006, and has held the status of a "Special Protection Area for Birds" (SPA) since 1990.

The hydrological cycle of the lagoon is influenced by precipitation and regulated by the Albufera Drainage Board, which surrounds its management to the demands of the surrounding rice cultivation [19].

Nonetheless, beginning in the 1970s, the introduction of nutrients through the canals conducted to eutrophication processes. This led to an increase in phytoplankton biomass, a decline in water transparency, and ultimately the disappearance of macrophyte meadows [20–22]. Assessments by Onandia et al. [23] reveal that the lagoon exhibits an average chlorophyll-a concentration ([Chl-a]) of 167 µg/L (ranging from 4 to 322 µg/L), Secchi disk depth (Z_{SD}) of 0.34 m (ranging from 0.18 to 1.0 m), total phosphorus concentrations of 155 µg/L (ranging from 41 to 247 µg/L), and total nitrogen concentration of 3.9 mg/L (ranging from 1.8 to 6.6 mg/L).

According to Romo et al. [24], the lagoon has notably transitioned into a turbid phase as conceptualized within Scheffer et al. [25] model of alternative states. Eutrophication emerges as the key factor driving this shift, attributed to the influx of nutrients through irrigation channels [21]. Consequently, this has resulted in a pronounced degradation of the wetland area [25].

Preprints (www.preprints.org) | NOT PEER-REVIEWED | Posted: 6 September 2023 doi:10.20944/preprints202309.0311.v1

2.2. Sampling and laboratory methods

During July and August 2018, July 2021, November 2021, in the period between March and December 2022 and between February and May 2023, weekly sampling was carried out in the Albufera of Valencia lagoon. During days with favorable weather conditions, boat trips were made to obtain samples at four specific points of the lake: "North", "Center", "South" and "Quay" (Figure 1). In addition, other points, such as P1 and P2, were sampled on occasion, depending on sampling interests.

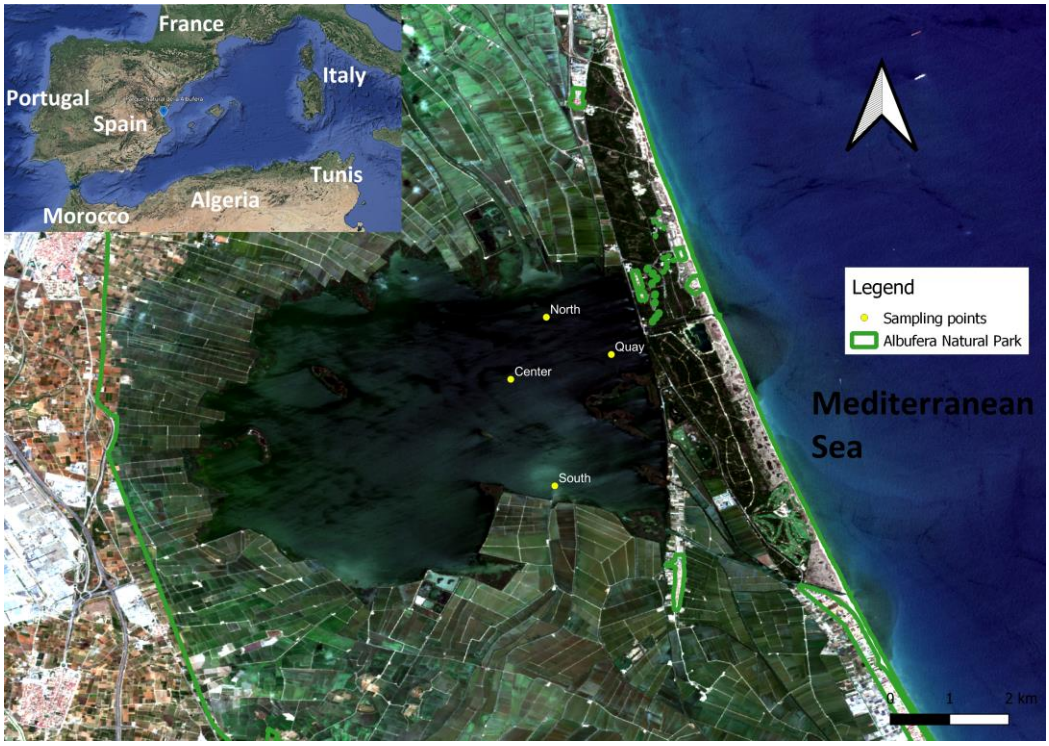

Figure 1. Location of field sampling points in the Albufera lagoon. Date of image from Sentinel-2: 24-june-2022. Processed using SNAP 8.0 and QGIS 3.22.

These samplings were scheduled to coincide on dates close to the acquisition of images by the S2A satellite, with a temporal difference of no more than 3 days, following the method proposed by Kutser [26]. During field sampling, measurements of water transparency, temperature and conductivity were performed, and samples were taken for subsequent calculation of [Chl-a] in the laboratory.

Water transparency was assessed by Secchi disk visibility depth, calculating the average between the depth at which the disk ceases to be visible from the surface and the depth at which it becomes visible again [27]. Water temperature and conductivity were measured using a portable handheld conductivity meter (Hanna Instruments).

Water samples collected in the field were filtered using 0.47 mm Whatman GF/F glass fiber filters. Chl-a was extracted from the filtered samples using a solvent solution prepared with dimethyl sulfoxide and 90% acetone following Shoaf and Lium [28]. The amount of extracted pigment was measured using a Beckman DU 640 spectrophotometer, and the calculation methodology proposed by Jeffrey and Humphrey [29] was used to determine [Chl-a].

2.3. Remote sensing imagery

The images employed for this research were sourced from the database of the European Space Agency (ESA) S2 mission. This mission is executed by two satellites, denoted as S2A and S2B, both outfitted with the Multispectral Instrument (MSI) sensor. The MSI sensor captures the Earth's reflected radiation across 13 distinct spectral bands (as detailed in Table 1), encompassing

Preprints (www.preprints.org) | NOT PEER-REVIEWED | Posted: 6 September 2023 doi:10.20944/preprints202309.0311.v1

wavelengths from the visible spectrum to the near and shortwave infrared. These bands feature varying spatial resolutions of 10, 20, and 60 meters [14].

Table 1. Sentinel-2A spectral bands. Data from ESA [14].

Band	Spectral region		Wavelength (nm)		Spatial resolution (m)
			Central	Wide	
B1	Visible	Deep blue	443	60	60
B2		Blue	490	10	10
B3		Green	560	10	10
B4		Red	665	10	10
B5		Red edge	705	20	20
B6			740	20	20
B7			783	20	20
B8	Near infrared (NIR)		842	115	10
B8a			865	20	20
B9	Short wavelength infrared (SWIR)		945	20	60
B10			1380	20	60
B11			1610	90	20
B12			2190	180	20

Even though the primary objective of the mission was to investigate vegetation, urban areas, and terrestrial ecosystems, the newly introduced red edge bands, enhanced radiometric quality, and the high spatial resolution of the MSI sensor have proven highly valuable for the analysis of inland waters [17].

We utilized images from the years 2018, 2021, and 2022, sourced from the ESA Copernicus Open Access Hub portal. We carefully selected images devoid of cloud cover that corresponded with lagoon field data. Our selection focused on images with the Sen2Cor atmospheric correction (level 2A), known to provide optimal reflectivity results in eutrophic waters, as exemplified in the case of the Albufera of Valencia [17,30]. A total of 21 images were considered suitable for subsequent analysis, comprising 5 from 2018, 3 from 2021, 9 from 2022, and 4 from 2023.

The processing of the selected 21 images was executed using the SNAP software (Brockmann Consult, Hamburg, Germany). Given the diverse resolution requirements of algorithms utilized in subsequent phases, it was necessary to resample the images to a 10-meter resolution through the interpolation tool integrated within SNAP. Consequently, we calculated reflectivity for each sampling point using a 3x3 pixel grid [26], utilizing the first seven bands of S2A (B1 to B7).

2.4. Algorithm retrieval

To calibrate the algorithms, first, optical models must be selected from which to perform operations with the S2 spectral bands and correlate these with the field data to develop an algorithm to validate. These models are based on the way in which solar radiation reflects on the water surface depending on the substances it contains (phytoplankton, suspended inorganic material and dissolved organic matter), since each of them scatters and reflects light differently [31].

When estimating Secchi disk depth, it's essential to recognize that transparency and other variables like chlorophyl-a and turbidity are inversely related. The impact of turbidity on the light intensity of water bodies is observable across the entire spectrum due to the absorption caused by optically active elements like chlorophyl-a, colored dissolved organic matter (CDOM), and other compounds [31]. The models selected to estimate the Z_{SD} in the previous studies (Table 2) were R490/R560, R490/R705 and R560/R705, so we need to understand the optical behavior of each of these bands.

 doi:10.20944/preprints202309.0311.v1

Table 2. Review of proposed models for estimating Secchi disk depth (Z_{SD}) in inland and coastal waters. Own elaboration and mathematical models obtained from the cited bibliography.

Model	References
R490/R560	Originally Mueller [32] and Giardino et al. [33]. Used by Delegido et al. [16] in reservoirs of the Jucar basin.
R490/R705	Originally Alikas and Kratzer [11]. Employed by Pereira-Sandoval et al. [15] in the Albufera of Valencia and reservoirs of the Jucar basin.
R560/R705	Originally Koponen et al. [31]. Sòria-Perpinyà et al. [17] in the Albufera of Valencia.

In the blue band (R490), the main phenomenon is the reflectivity of water, which decreases with the presence of suspended matter [34]. Then, in the green band (R560), there is a minimum absorption of the combination of photosynthetic pigments [35], suspended particles and CDOM [36]. Finally, in the red band (R705), [Chl-a] has a reflectivity peak at 700 nm, which will be higher the higher its concentration, related to light scattering and absorption by phytoplankton [37] and its fluorescence maximum at 683 nm [38]. However, the impact of pigments is minimal at 705 nm, where the primary phenomenon is the backscattering caused by phytoplankton [35]. This is also influenced by near-infrared scattering originating from suspended particles, even though water absorption continues within this wavelength band [12].

Following the completion of image processing and the calculation of mean values for each spectral band at every sampling point, these outcomes were utilized in conjunction with an Excel spreadsheet (Microsoft Corporation, Redmond WA, USA). This allowed for the execution of the required operations using the pre-selected model.

Outliers were subsequently eliminated, and 70% of the data was randomly allocated for the calibration process, with the remaining 30% preserved for validation purposes. Throughout the model calibration phase, a linear regression analysis was conducted between each optical model and the Z_{SD} data obtained during field measurements. The calculation of Pearson's coefficient of determination (R^2) was performed, and the equation of the regression line was established. This equation indicates the adjusted algorithm, which will subsequently serve for validation purposes.

2.5. Data analysis

Once the algorithm with the highest R^2 was selected, its validity in the estimates was evaluated by means of a new linear regression between the values estimated by this algorithm for Z_{SD} and the data obtained in the field. It was plotted on a 1:1 graph and the p-value and the root mean square error (RMSE), normalized root mean square error (NRMSE), mean absolute error (MAE) and normalized mean absolute error (NMAE) were calculated. In addition, thematic maps of Z_{SD} were generated by applying the validated equation to 4 of the 21 cloud-free images of the period considered using the Sentinel Application Program (SNAP) software to show the spatiotemporal evolution of the lagoon.

3. Results

3.1. Field and laboratory data

The average temperature recorded was 23.3°C, ranging from 11.5°C at the "quay" point on 4 April 2022, to 30.3°C on 11 July 2022, also at the same point. The standard deviation of the temperature was 5.8°C. For conductivity, the average was 1870 µS/cm, with a range that varied between 1031 µS/cm on 10 May 2022, at the "P1" point and 3040 µS/cm at the "north" point on 15 July 2018. The standard deviation was 575 µS/cm.

Regarding the Z_{SD}, an average of 0.31 m was observed, fluctuating between 0.15 m on 5 May 2023, at the "quay" point and on 16 May 2023, at the "north", "quay" and "P2" points, and 0.55 m on 15 July 2018, at the "P1" point. The standard deviation was 0.09 m.

Preprints (www.preprints.org) | NOT PEER-REVIEWED | Posted: 6 September 2023 doi:10.20944/preprints202309.0311.v1

Regarding chlorophyll-a concentration, a mean value of 164.3 mg/m^3 was obtained, with a range that varied between 21.0 mg/m^3 detected on 20 April 2022, at the "south" point, and 376.0 mg/m^3 detected on 6 June 2022, at the "center" point. The standard deviation was 88.5 mg/m^3, indicating a high spatiotemporal variability in the values.

3.2. Algorithm retrieval and validation

Table 3 shows the equations resulting from the calibration of the models for the Z_{SD} variable. The equation that has been selected due to its high correlation coefficient is the first one.

Table 3. Results of the calibration of the algorithms for the estimation of the Secchi disk depth in the Albufera. In the equations, "y" represents the Z_{SD} and "x" the corresponding model. The selected model with a higher coefficient of determination is indicated with *.

Model	Algorithm	R^2
R560/R705	y = 0,4242 x + 0,0577 *	0,6149
R490/R705	y = 0,3944 x + 0,1246	0,2805
R490/R560	y = -0,0455 x + 0,3426	0,0043

In the table above, we observe how the R490/R560 model, which was originally designed for clear water does not reach an R^2 greater than 0.1. The R490/R705 and R560/R705 models, which are more suitable for more turbid waters, obtain higher values of this statistic. The R560/R705, which has the highest value, as shown in Figure 2, where the graphs of the calibration and validation of the selected algorithm, are presented. As we can see in Figure 2A, a coefficient of determination of 0.6149 was obtained in the calibration and 0.916 in the validation with the field data (Figure 2B), showing a clear correlation between the estimated and field data. A p-value < 0.001 was obtained.

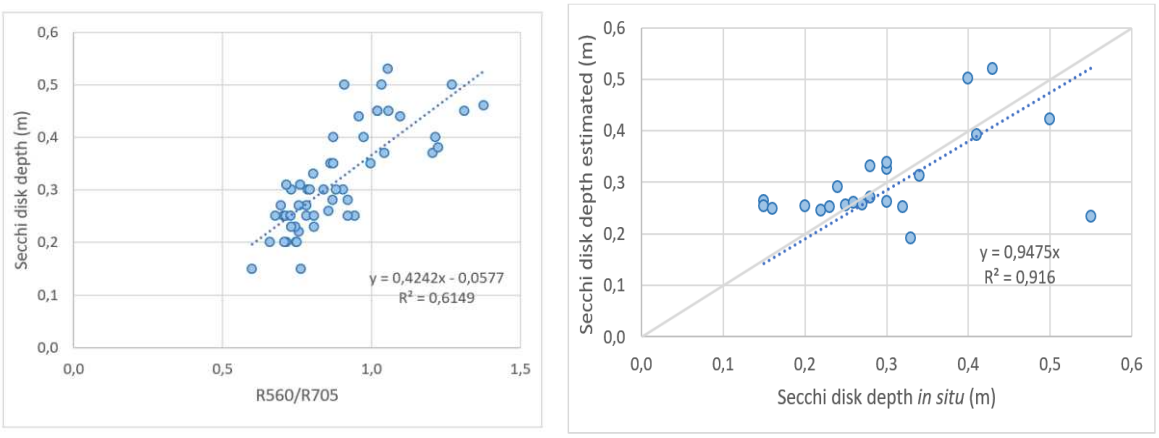

(**a**) (**b**)

Figure 2. (**a**) Calibration of the R560/R705 model to estimate transparency in the Albufera; (**b**) Validation of the R560/R705 model for transparency in the Albufera.

Therefore, the equation obtained for the estimation of the Z_{SD} in the Albufera using the S2 images is as follows:

$$Z_{SD}\ (m) = 0.4242 \times R560/R705 + 0.0577 \quad (1)$$

Table 4 shows the statistics compared between the previous algorithm, obtained from 2017 Albufera Z_{SD} data, and that of the present study, obtained with data from 2018 to 2023. In both cases, errors have been calculated from estimates made for images from 2018 to 2023.

Table 4. Comparative statistics of the validation of the algorithms developed in the present study and the previous study. Statistics have been calculated from 2018-23 field data.

Preprints (www.preprints.org) | NOT PEER-REVIEWED | Posted: 6 September 2023 doi:10.20944/preprints202309.0311.v1

Algorithm	RMSE	NRMSE	MAE	NMAE	Reference of the algorithm
y = 0.4242 × R560/R705 + 0.0577	0.07 m	17.8%	0.05 m	13.37%	This study
y = 0.224 × R560/R705 + 0.0836	0.08 m	20.7%	0.06 m	14.92%	Sòria-Perpinyà et al. [17]

Therefore, the algorithm developed in the present study has demonstrated its validity for estimating the Z_{SD} (m) of the Albufera of Valencia, reducing the RMSE in its estimates to below 20%, thus proving to be more accurate than the previously developed algorithm.

3.3. Thematic maps

Applying equation (1) derived in the present study, we analyzed images representing the study period (2018-2023). By processing them, we generated thematic maps illustrating the evolution of the variable under study.

Figure 3 presents maps of Z_{SD} at key moments in 2022, exposing its seasonal variation. Lower Z_{SD} values, associated with periods of higher chlorophyll-a, indicate lower transparency. In contrast, increases in Z_{SD} are related to decreases in chlorophyll-a, highlighting the inverse relationship between these variables throughout the year.

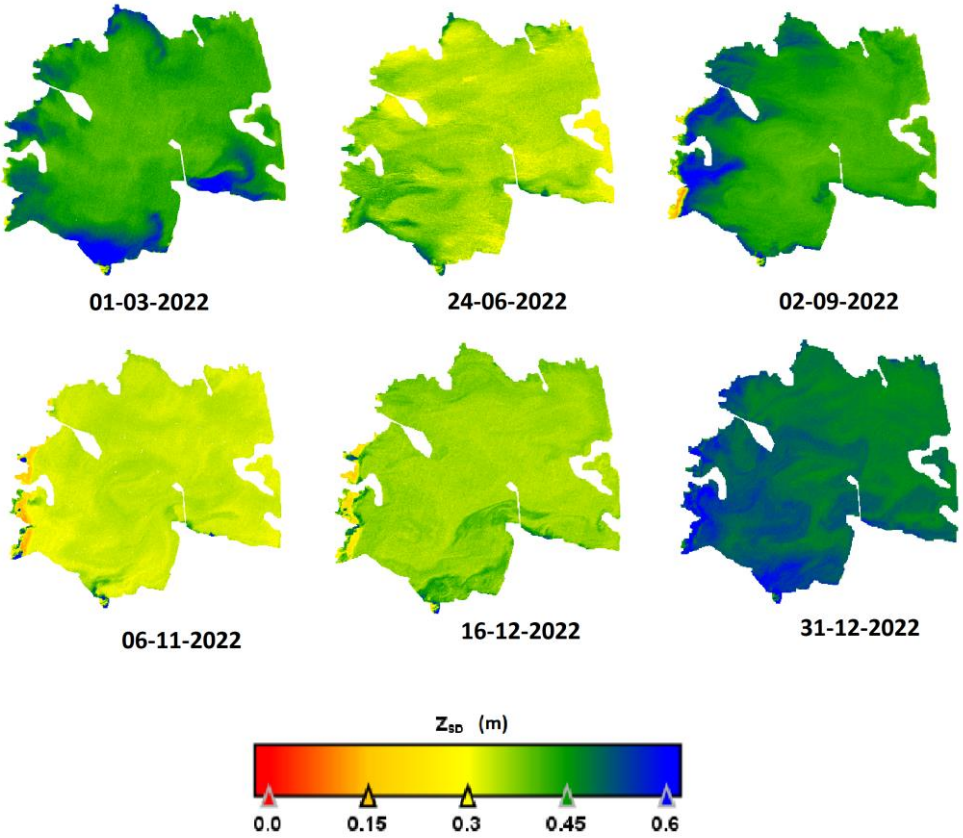

Figure 3. Thematic maps showing spatiotemporal variation of Secchi Disk Depth (Z_{SD}) in some moments of 2022 in the Albufera lagoon. Maps processed using SNAP 8.0.

The highest Z_{SD} values are observed between January and March, when water clarity increases due to reduced chlorophyll-a concentration resulting from the drainage of rice fields at the end of winter. These water inputs to the lagoon and the opening of floodgates intensify aquatic renewal. From May to June, there is a decreasing transparency due to the first seasonal peak of chlorophyll-a,

 doi:10.20944/preprints202309.0311.v1

due to the decrease in the renewal rate due to rice water inputs during planting and the closing of floodgates that connect to the Mediterranean Sea.

During the end of the summer, transparency increases again, coinciding with the second annual minimum of chlorophyll-a due to nutrient depletion, starting at the shores, where water volume is lower, expanding later towards the center.

Between November and the beginning of December, water clarity decreases again due to the increase in algal turbidity due to the contribution of nutrient waters from the rice field, which is flooded as a wetland. This process begins on the shores and spreads towards the interior of the lagoon. At the end of December, the water clarity increases again, to return to the initial situation.

4. Discussion

Starting with the mathematical fits of the algorithms for the Z_{SD} variable, it is important to highlight the inadequacy of the R490/R560 model, calibrated by Mueller [32] and Giardino et al. [33] for very clear ocean waters, in the context of the Albufera. This lagoon is characterized as hypertrophic, which implies the presence of high levels of nutrients and suspended material in the water. Therefore, it is not surprising that this model does not work properly, since it was designed for very different marine environments in terms of transparency.

Likewise, the R490/R705 model, which has shown good results in Nordic lakes, coastal areas of the Baltic Sea and reservoirs of the Valencian Community in previous studies, fails to obtain such a high coefficient in the study carried out in the Albufera. The difference lies in the fact that the previous studies covered a wide range of lakes, from oligotrophic to eutrophic, while in the case of the Albufera it is exclusively a hypertrophic lagoon. This distinction is relevant because of the variations in water composition and quality between these different types of water bodies, which affects the accuracy of the models.

One aspect to consider is the reflectivity of water in the 490 nm band, which decreases with the presence of suspended solids and high turbidity values, a common phenomenon in the Albufera. Sebastiá-Frasquet et al. [34] highlighted this fact in their study, which explains why models based on the R490 band as numerator do not obtain good results in this lagoon. These results support the need to select more suitable models to estimate the Z_{SD} in turbid and highly eutrophic waters such as the Albufera.

In the study conducted in the Albufera, the R560/R705 model, successfully calibrated for Finnish turbid lakes in the work of Koponen et al. [31], shows better coefficients, coinciding with the results obtained by Sòria-Perpinyà et al. [17]. The choice of this model is based on the similarity of the Albufera with the lakes where the original calibration was performed, in terms of eutrophication. In addition, the use of the 560 nm band in this model is beneficial, since in that band there is a minimum of light absorbance by pigments, colored dissolved organic matter (CDOM) and suspended solids. This has been corroborated in previous studies, such as those of Delegido et al. [35] and Gurlin et al. [36] and who found a lower influence of absorption in the 560 nm band due to the presence of these components in water.

In addition, a reduction in the statistical error in the estimation values of the algorithm calibrated and validated in the present study was achieved compared to those obtained by the algorithm developed in the research conducted by Sòria-Perpinyà et al. [17], in relation to the field data covered in the period 2018-23. This discrepancy can be explained by the fact that the previous algorithm was calibrated based on in situ Z_{SD} data collected in 2017 in the Albufera, which presented a range between 0.19 and 0.62 m with an average of 0.33 m, while in the present study values ranging between 0.15 and 0.52 m were obtained, with an average of 0.31 m. Consequently, it is deduced that water transparency has experienced a marginal reduction in the Albufera during the period 2018-23 compared to 2017, leading to a decrease in the Z_{SD}. This reduction has consequently contributed to a loss of accuracy in the previous algorithm in favor of the new one.

Finally, the application of remote sensing in this study has proven to be of great relevance by providing a broad perspective on the spatiotemporal heterogeneity of water bodies, in this case, the Albufera lagoon. The ability to acquire information continuously and over wide areas over time has

made it possible to capture variations in the Secchi Disk Depth (Z_{SD}) and its relationship with the evolution of the lagoon state [22]. In contrast to traditional point sampling techniques, which would be costly and limited in terms of coverage, remote sensing has provided a comprehensive view of changes in lagoon water quality. This approach has allowed a more complete understanding of seasonal and spatial patterns, providing essential information for environmental monitoring, demonstrating the applications of remote sensing as a key tool in the management of natural areas.

5. Conclusions

To sum up, the results of this study highlight the inadequacy of the R490/R560 and R490/R705 models, originally designed for clear ocean waters and lakes of different trophic states, respectively, for estimating the Z_{SD} in Albufera, a hypertrophic lagoon with high levels of suspended solids and turbidity. In contrast, the R560/R705 model, calibrated for turbid lakes like Albufera, presents better coefficients and a higher correlation between estimated data and field data. These results support the need to select appropriate models and consider the specific characteristics of the water bodies when developing algorithms for estimating the Z_{SD}. The final equation obtained in this study for estimating the Z_{SD} in the Albufera has been an improvement of the previous algorithm, with a higher coefficient of determination and a lower statistical error compared to the previous approach. In addition, the application of remote sensing in this study has provided a broad perspective of the spatiotemporal variability of water transparency in the Albufera lagoon, as opposed to traditional sampling methods, and has demonstrated its potential as an environmental management tool.

Author Contributions: Conceptualization and methodology design, J.V.M. and J.M.S.; Field and laboratory work, all authors; Data curation, J.V.M. and J.M.S.; writing—original draft preparation, J.V.M.; writing—review and editing, all authors. All authors have read and agreed to the published version of the manuscript.

Funding: This research received no external funding.

Institutional Review Board Statement: Not applicable.

Informed Consent Statement: Not applicable.

Data Availability Statement: Images are available at ESA Copernicus Hub and the data presented are available on request from the corresponding author.

Conflicts of Interest: The authors declare no conflict of interest.

References

1 Matthews, M.W. A current review of empirical procedures of remote sensing in inland and near coastal transitional waters. *Int. J. Remote. Sens.* **2011**, *32(21)*, 6855-6899.
2 French, R.H.; Cooper, J.J.; Vigg, S. Secchi Disc Relationships. *J. Am. Water Resour. Assoc*. **1982**, *18*, 121–123.
3 Duntley, S.Q. The Visibility of Submerged Objects; Final Report to Office of Naval Research; Visibility Laboratory, Massachusetts Institute of Technology: Cambridge, MA, USA, 1952.
4 Preisendorfer, R.W. Secchi disk science: Visual optics of natural waters. *Limnol. Oceanogr.* **1986**, *31*, 909–926.
5 Lee, Z.; Shang, S.; Qi, L.; Yan, J. Estimation of Secchi-disk Depth Semi-analytically from Landsat-8 Data. *American Geophysical Union* **2016**, HI34A-1797.
6 Testa, J.M.; Lyubchich, V.; Zhang, Q. Patterns and trends in Secchi disk depth over three decades in the Chesapeake Bay estuarine complex. *Estuaries Coasts* **2019**, *42*, 927–943.
7 Doron, M.; Babin, M.; Hembise, O.; Mangin, A.; Garnesson, P. Ocean transparency from space: Validation of algorithms using MERIS, MODIS and SeaWiFS data. *Remote Sens. Environ.* **2011**, *115*, 2986–3001.
8 Lindell, T.; Pierson, D.; Premazzi, G. Manual for Monitoring European Lakes Using Remote Sensing Techniques. Office for Official Publications of the European Communities, Luxembourg, 1999, 164 pp.
9 Olmanson, L.G.; Bauer, M.E.; Brezonik, P.L. A 20-year Landsat water clarity census of minnesota's 10,000 lakes. *Remote Sens. Environ.* **2008**, *112*, 4086–4097.
10 Vollenweider, R. A., & Kerekes, J. Eutrophication of Waters: Monitoring. Assessment and Control. OECD, Paris. 1982. 154 pp.
11 Alikas, K.; Kratzer, S. Improved retrieval of Secchi depth for optically-complex waters using remote sensing data. *Ecol. Indic.* **2017**, *77*, 218–227.

12 Caballero, I.; Roca, M.; Santos-Echeandía, J.; Bernárdez, P.; Navarro, G. Use of the Sentinel-2 and Landsat-8 Satellites for Water Quality Monitoring: An Early Warning Tool in the Mar Menor Coastal Lagoon. *Remote Sens*. **2022**, 14, 2744. https://doi.org/10.3390/rs14122744.

13 Navalgund, R.R.; Jayaraman, V.; Roy, P.S. Remote sensing applications: An overview. *Curr. Sci.* **2007**, *93*, 1747–1766.

14 European Spacial Agency (ESA). Sentinel-2: ESA's Optical High-Resolution Mission for GMES Operational Services. K. Fletcher (ed.). ESA Communications, Noordwijk. The Netherlands, 2012, 77 pp.

15 Pereira-Sandoval, M.; Urrego, E.P.; Ruiz-Verdu, A.; Tenjo, C.; Delegido, J.; Soria-Perpinya, X.; Vicente, E.; Soria, J.M.; Moreno, J. Calibration and validation of algorithms for the estimation of chlorophyll-a concentration and Secchi depth in inland waters with Sentinel-2. *Limnetica* **2019**, *38(1)*, 471-487.

16 Delegido, J.; Urrego, P.; Vicente, E.; Sòria-Perpinyà, X.; Soria, J.M.; Pereira-Sandoval, M.; Ruiz-Verdú, A.; Peña, R.; Moreno, J. Turbidez y profundidad de disco de Secchi con Sentinel-2 en embalses con diferente estado trófico en la Comunidad Valenciana. *Rev Teledec.* **2019**, *54*, 15–24.

17 Sòria-Perpinyà, X.; Urrego, E.P.; Pereira-Sandoval, M.; Ruiz-Verdú, A.; Soria, J.M.; Delegido, J.; Vicente, E.; Moreno, J. Monitoring Water Transparency of a Hypertrophic Lake (The Albufera of València) Using Multitemporal Sentinel-2 Satellite Images. *Limnetica* **2020**, *39*, 373–386.

18 Soria, J.; Vicente, E.; Miracle, M. The Influence of Flash Floods on the Limnology of the Albufera of Valencia Lagoon (Spain). *SIL Proc.* **2000**, *27*, 2232–2235.

19 Soria, J.; Vera-Herrera, L.; Calvo, S.; Romo, S.; Vicente, E.; Sahuquillo, M.; Sòria-Perpinyà, X. Residence Time Analysis in the Albufera of Valencia, a Mediterranean Coastal Lagoon, Spain. *Hydrology* **2021**, *8*, 37.

20 Martín, M.; Oliver, N.; Hernández-Crespo, C.; Gargallo, S.; Regidor, M.C. The use of free water surface constructed wetland to treat the eutrophicated waters of lake L'Albufera de Valencia (Spain). *Ecological Engineering* **2013**, *50*, 52-61. https://doi.org/10.1016/j.ecoleng.2012.04.029

21 del Barrio Fernández, P.; Gómez, A.G.; Alba, J.G.; Díaz, C.Á.; Cortezón, J.A.R. A model for describing the eutrophication in a heavily regulated coastal lagoon. Application to the Albufera of Valencia (Spain). *J. Environ. Manage.* **2012**, *112*, 340-352. https://doi.org/10.1016/j.jenvman.2012.08.019

22 Martín, M.; Hernández-Crespo, C.; Andrés-Doménech, I.; Benedito-Durá, V. Fifty years of eutrophication in the Albufera lake (Valencia, Spain): Causes, evolution and remediation strategies. *Ecological Engineering* **2020**, *155*, 105932. https://doi.org/10.1016/j.ecoleng.2020.105932

23 Onandia, G.; Gudimov, A.; Miracle, M.R.; Arhonditsis, G. Towards the development of a biogeochemical model for addressing the eutrophication problems in the shallow hypertrophic lagoon of Albufera de Valencia, Spain. *Ecol. Inf.* **2015**, *26*, 70-89.

24 Romo, S.; García-Murcia, A.; Villena, M.J.; Sanchez, V.; Ballester, A. Phytoplankton trends in the lake of Albufera de Valencia and implications for its ecology, management, and recovery. *Limnetica* **2008**, *27*, 11–28.

25 Scheffer, M.; Hosper, S.H.; Meijer, M.L.; Moss, B.; Jeppesen, E. Alternative equilibria in shallow lakes. *Trends Ecol. Evol.* **1993**, *8(8)*, 275-279.

26 Kutser, T. The possibility of using the Landsat image archive for monitoring long time trends in coloured dissolved organic matter concentration in lake waters. *Remote Sens. Environ.* **2012**, *123*, 334-338.

27 Wetzel, R.G.; G.E. Likens. Limnological Analyses. (3rd edition). Springer, New York, 2000, 429 pp.

28 Shoaf, W. T.; Lium, B. W. Improved extraction of chlorophyll a and b from algae using dimethyl sulfoxide. *Limnol. Oceanogr.* **1976**, *21(6)*, 926-928.

29 Jeffrey, S. T.; Humphrey, G. F. New spectrophotometric equations for determining chlorophylls a, b, c1 and c2 in higher plants, algae and natural phytoplankton. *Biochem. Physiol. Pflanz.* **1975**, *167(2)*, 191-194.

30 Ruescas, A.B.; Pereira-Sandoval, M.; Tenjo, C.; Ruiz-Verdú, A.; Steinmetz, F.; Keukelaere, L.D. Sentinel-2 Atmospheric Correction inter-comparison over two lakes in Spain and Peru-Bolivia. In Proceedings of the Colour and Light in the Ocean from Earth Observation (CLEO), ESA-ESRIN, Frascati, Italy, 6–8 September 2016.

31 Koponen, S.; Pulliainen, J.; Kallio, K.; Hallikainen, M. Lake water quality classification with airborne hyperspectral spectrometer and simulated MERIS data. *Remote Sens. Environ.* **2002**, *79(1)*, 51-59.

32 Mueller, J.L. SeaWIFS algorithm for the diffuse attenuation coefficient, k(490), using water-leaving radiances at 490 and 555 nm. In SeaWiFS postlaunch Calibration and Validation Analyses; BiblioGov: Columbus, OH, USA, 2000; Volume 3, pp. 24–27.

33 Giardino, C.; Bresciani, M.; Cazzaniga, I.; Schenk, K.; Rieger, P.; Braga, F.; Matta, E.; Brando, V.E. Evaluation of multi-resolution satellite sensors for assessing water quality and bottom depth of lake Garda. *Sensors* **2014**, *14*, 24116–24131.

34 Sebastiá-Frasquet, M.-T.; Aguilar-Maldonado, J.A.; Santamaría-Del-Ángel, E.; Estornell, J. Sentinel 2 Analysis of Turbidity Patterns in a Coastal Lagoon. *Remote Sens*. **2019**, *11*, 2926. https://doi.org/10.3390/rs11242926

35 Delegido, J.; Tenjo, C.; Ruiz-Verdú, A.; Peña, R.; Moreno, J. Modelo empírico para la determinación de clorofila-a en aguas continentales a partir de los futuros Sentinel-2 y 3. Validación con imágenes HICO. *Rev. Teledetec.* **2014**, *41*, 37–47.
36 Gurlin, D.; Gitelson, A.A.; Moses, W.J. Remote sensing of chl-a concentration in turbid productive waters—Return to a simple two-band NIR-red model? *Remote Sens. Environ.* **2011**, *115*, 3479–3490.
37 Morel, A.; Prieur, L. Analysis of variations in ocean color. *Limnol. Oceanogr.* **1977**, *22*, 709–722.
38 Smith, R.C.; Baker, K.S. Optical classification of natural waters. *Limnol. Oceanogr.* **1978**, *23*, 260–267.